PROCEEDINGS OF THE ROYAL SOCIETY B

rspb.royalsocietypublishing.org

Research

Cite this article: Duncan AB, Gonzalez A, Kaltz O. 2013 Stochastic environmental fluctuations drive epidemiology in experimental host–parasite metapopulations. Proc R Soc B 280: 20131747.
http://dx.doi.org/10.1098/rspb.2013.1747

Received: 5 July 2013
Accepted: 23 July 2013

Subject Areas:
ecology, health and disease and epidemiology, evolution

Keywords:
host–parasite, epidemiology, variation, red noise, spatial synchrony

Authors for correspondence:
Alison B. Duncan
e-mail: alison.duncan@univ-montp2.fr
Andrew Gonzalez
e-mail: andrew.gonzalez@mcgill.ca
Oliver Kaltz
e-mail: oliver.kaltz@univ-montp2.fr

Electronic supplementary material is available at http://dx.doi.org/10.1098/rspb.2013.1747 or via http://rspb.royalsocietypublishing.org.

Royal Society Publishing
Informing the science of the future

Stochastic environmental fluctuations drive epidemiology in experimental host–parasite metapopulations

Alison B. Duncan[1], Andrew Gonzalez[2] and Oliver Kaltz[1]

[1]Institut des Sciences de l'Evolution de Montpellier (ISEM), UMR 5554, Université Montpellier 2, Place Eugene Bataillon, 34095, Montpellier Cedex 05, France
[2]Department of Biology, McGill University, 1205 Docteur Penfield Avenue, Montreal, Quebec, Canada H3A 1B1

Environmental fluctuations are important for parasite spread and persistence. However, the effects of the spatial and temporal structure of environmental fluctuations on host–parasite dynamics are not well understood. Temporal fluctuations can be random but positively autocorrelated, such that the environment is similar to the recent past (red noise), or random and uncorrelated with the past (white noise). We imposed red or white temporal temperature fluctuations on experimental metapopulations of *Paramecium caudatum*, experiencing an epidemic of the bacterial parasite *Holospora undulata*. Metapopulations (two subpopulations linked by migration) experienced fluctuations between stressful (5°C) and permissive (23°C) conditions following red or white temporal sequences. Spatial variation in temperature fluctuations was implemented by exposing subpopulations to the same (synchronous temperatures) or different (asynchronous temperatures) temporal sequences. Red noise, compared with white noise, enhanced parasite persistence. Despite this, red noise coupled with asynchronous temperatures allowed infected host populations to maintain sizes equivalent to uninfected populations. It is likely that this occurs because subpopulations in permissive conditions rescue declining subpopulations in stressful conditions. We show how patterns of temporal and spatial environmental fluctuations can impact parasite spread and host population abundance. We conclude that accurate prediction of parasite epidemics may require realistic models of environmental noise.

1. Introduction

Increasingly, environmental variability is seen as an important factor driving host–parasite interactions [1–3]. Empirical and theoretical studies indicate that temporal environmental fluctuations are linked to disease severity, and can be key for accurate prediction of epidemic onset in natural populations of both animal and plant parasites [4–6]. However, not all parasites follow straightforward seasonal dynamics [7], and not all relevant environmental factors vary in a predictable fashion [8]. Hence, it remains an open question how environmental stochasticity drives epidemiological dynamics [7,9,10]. This is particularly important, as global climate change is expected to shift patterns of environmental variability [11].

The predictability of environmental fluctuations across temporal scales (i.e. diurnal, seasonal, annual) can be described by their autocorrelation structure. Natural environmental fluctuations tend to be positively autocorrelated ('red noise'), where current conditions are similar to those of the recent past [12], as opposed to uncorrelated random fluctuations ('white noise'), where current conditions are not similar to the recent past. Previous research has shown that noise structure can affect population dynamics and persistence [13]. One important prediction is that red noise favours the persistence of sink populations (populations with a negative intrinsic rate of growth) when fluctuations include transient periods in permissive conditions that allow growth and population recovery [14]. Similar outcomes are expected in a metapopulation context, but here conditions for long-term persistence are also determined by noise synchrony

across subpopulations. Asynchronous environmental noise reduces synchrony in subpopulation density fluctuations [15]. This can enhance the beneficial effects of red noise and promote metapopulation persistence, because migration from subpopulations at higher densities can rescue subpopulations at lower densities [16,17].

The relevance of these findings for epidemiology in host–parasite systems is unclear. Theoretical models indicate that temporal environmental stochasticity increases parasite population fluctuations, which may impede the spread of an epidemic, or increase parasite extinction risk [10,18,19]. However, we are aware of only one model that explicitly considers the importance of noise colour, and shows that red noise modifies the magnitude of parasite fluctuations [18]. Experimental manipulation of noise colour in the presence of parasites shows that blue noise (negatively correlated variation), in contrast to white, increases host resistance [20], and that low environmental disturbance frequency (approximating red noise) can enhance host population diversity [21]. However, experimental studies that track the long-term dynamics of hosts and their parasites in stochastic environments are lacking.

Time-series analyses of metapopulations often find that parasite epidemics are synchronized across cities or countries [22–24], which may be caused by shared stochastic climatic conditions ('environmental forcing'). Indeed, synchronized onset and periodicity of cholera epidemics across five different countries has been linked to the common occurrence of rainfall [23]. These observations point to the importance of integrating both the temporal and spatial pattern of environmental noise when studying parasite epidemiology in spatially structured populations.

We investigated the impact of red versus white environmental noise on host–parasite dynamics, using experimental metapopulations of the ciliate *Paramecium caudatum* infected with the bacterial parasite *Holospora undulata*. We imposed daily temperature fluctuations, between permissive (23°C) and restrictive (5°C) conditions, following red or white temporal sequences. We predicted that initially the parasite and host would benefit from red noise, because it would produce longer periods at 23°C, which is more favourable for population growth [25,26]. Red noise was expected to benefit the parasite directly if its demographic response to the noise was similar to *P. caudatum*. In addition, red noise may benefit the parasite indirectly, because larger host population sizes favour increased parasite transmission.

As we were also interested in the combined effects of temporal and spatial noise structure, we manipulated the synchrony of red or white temperature sequences between subpopulations. Thus, we exposed subpopulations within a metapopulation to the same ('synchronous temperatures') or different ('asynchronous temperatures') temperature sequences. We expected the beneficial effects of red noise for host and parasite to be maximal under asynchronous temperatures, because large subpopulations brought about by permissive conditions (23°C) may rescue those experiencing stressful conditions, an effect previously demonstrated for single-species populations [16].

2. Methods

(a) Study organisms

Paramecium caudatum is a freshwater ciliate that feeds on bacteria and detritus [27]. It is found in still water bodies throughout the Northern Hemisphere. In laboratory conditions, *Paramecium* is maintained in Volvic mineral water with dried organic lettuce, supplemented with the bacterium *Serratia marcescens* as food [28]. Reproduction is predominantly asexual through mitotic division. Optimal temperature conditions are around 28–30°C, with maximum and minimum tolerated temperatures of 32–36°C and 2–6°C, respectively [26]. At temperatures of around 4°C, *Paramecium* growth is almost entirely arrested for the *Paramecium* clone used in this study. In their natural environment, *P. caudatum* are found at the edge of small water-bodies, so are likely to be exposed to frequent temperature changes [29]. However, because this study tests ecological theory, it does not aim to represent the specific abiotic conditions that *Paramecium* and *Holospora* encounter in their natural habitat.

Holospora undulata, a Gram-negative α-proteobacterium, is a natural parasite of *P. caudatum*. *Paramecium* ingest infectious forms (15–20 µm) during feeding [30], which are transferred to the micronucleus following fusion with food vesicles containing the parasite. Infectious forms differentiate into reproductive forms (5 µm) approximately 24 h later, which then begin to multiply. After 7–10 days, an accumulation of reproductive forms is followed by the production of infectious forms [31]. Both morphotypes can be present simultaneously in the micronucleus. Vertical transmission occurs when reproductive forms are transferred to the daughter micronuclei of cells following mitotic division. Horizontal transmission arises when infectious forms are released into the environment during cell division or following host death. Thus, following initial infection, infected *Paramecium* become infectious, in that they are able to transmit horizontally, after about a week. Parasite infection increases host mortality and reduces growth [32–34]. Optimal temperature for parasite development is between 23 and 30°C [25]. At low temperatures (less than or equal to 10°C), *Paramecium* can still become infected, but subsequent parasite within-host development or differentiation of transmission stages are stopped [25].

(b) Host and parasite origins

Paramecium clone *VEN* [32] was used in this experiment. Three months prior to the experiment, we seeded a mass culture of this clone from a single individual. The culture was stored at 23°C in 50 ml Falcon tubes and grown up by doubling the volume three times a week with fresh medium. Twenty-four hours before starting the experiment, the culture was mixed in a large Erlenmeyer flask. On day 1 of the experiment, the mass culture was diluted with medium to a density of 250 *Paramecium* per millilitre. At the same time, we added infected individuals of the same clone to a portion of the uninfected mass culture to create an infected mass culture, with the same density and an infection prevalence of 5%. The infected individuals were taken from a 100% infected culture, established from a single infected *VEN* individual. This infected individual had been isolated from another mass culture infected with a mix of isolates from our laboratory (see [35]).

(c) Main experiment

The infected and uninfected *Paramecium* mass cultures were each distributed across 50 ml Falcon tubes in 30 ml volumes. A replicate metapopulation comprised two 50 ml Falcon tubes (referred to as subpopulations) linked by liquid transfer to create high (6.67% of total culture volume) or low (0.67% of total culture volume) levels of migration. In infected metapopulations, one of the two subpopulations was seeded from the infected mass culture.

We imposed two variable temperature treatments in a factorial design. In the noise colour treatment, metapopulations were exposed to temperature fluctuations between 5 and 23°C, following red or white noise patterns. In the temperature synchrony treatment, subpopulations within a metapopulation experienced

perfectly synchronous or spatially uncorrelated temperature fluctuations (see below). Four infected and four uninfected metapopulations were randomly assigned to each of the four treatment combinations, resulting in a total of 64 metapopulations (2 parasite × 2 noise colour × 2 temperature synchrony × 2 levels of migration × 4 replicates).

(i) Noise colour

Temporal variation involved alternating populations daily between 5 and 23°C following 'red' or 'white' sequences, over a 56-day period. All subpopulations had 28 days at 23°C and 28 days at 5°C, experiencing an overall mean temperature of 14°C. White noise sequences were created using randomly generated number sequences. Fisher's kappa spectral density tests were used to ensure no serial autocorrelation in the ordering of days ($p > 0.10$). Red noise sequences were created using a function ensuring a serial correlation of 0.8 in the sequence. Fisher's kappa spectral density tests were used to ensure serial autocorrelation in the ordering of days ($p < 0.01$). Each subpopulation received its own sequence, except for the temperature synchrony treatment, where both subpopulations followed the same sequence (see the electronic supplementary material, figure S1a for *Paramecium* densities in relation to temperature sequences, for example metapopulations). Subpopulations following red noise sequences experienced a mean of 10.31 (±0.34 s.e.) temperature shifts, and populations following white sequences 28.34 (±0.47 s.e.) temperature shifts, during the 56-day experiment.

(ii) Temperature synchrony

In the temperature synchrony treatment, we manipulated the similarity of temporal temperature fluctuations within a metapopulation. 'Synchronous' temperature fluctuations occurred when subpopulations within a metapopulation shared the same temporal sequences (temperature sequences were perfectly correlated; $r = 1$). 'Asynchronous temperatures' occurred when subpopulations experienced uncorrelated temperatures, as each subpopulation within the metapopulation was allocated a different temporal sequence (mean temperature correlation coefficient between subpopulation sequences $= -0.03 \pm 0.02$; $t = 1.41$, d.f. $= 31$, $p = 0.17$; electronic supplementary material, figure S1).

(iii) Culling and migration

Every 4 days, 6 ml of each subpopulation was removed and replaced with fresh medium. Standard *Paramecium* culturing techniques entail frequent dilution to maintain microcosm populations under continuous growth conditions [33]. We imposed elevated culling to accentuate population decline, because we tested theory that predicts red noise is beneficial for sink populations [14,16,17]. After day 28, we increased culling to every 2 days to increase the rate of decline. Migration between subpopulations occurred following each culling event and prior to the addition of fresh culture medium. Migration entailed transferring either 2 ml (6.67%) or 200 µl (0.667%) between subpopulations every 4 days.

(iv) Constant-temperature control treatment

Additional infected and uninfected control metapopulations were established to monitor *Paramecium* and parasite dynamics in constant environments. Control metapopulations were assigned to constant temperatures of 5 and 23°C to confirm that these environments corresponded to restrictive and permissive conditions. These control metapopulations were also subject to high (6.67%) and low (0.67%) levels of migration (2 parasite × 2 temperatures × 2 migration × 4 replicates = 32 control metapopulations).

(v) Measurements

We measured population density every 4 days and infection prevalence every 8 days, by performing counts on the 6 ml removed from the subpopulations using a stereomicroscope. Infection prevalence was estimated from lacto–aceto–orcein fixations [31] of ≈40 *Paramecium* where possible, and never fewer than five. Their infection status was determined at a magnification of 1000× (phase contrast) and infection prevalence taken as the proportion of infected individuals in the sample.

(d) Statistical analysis

(i) Parasite dynamics

We used a general linearized mixed model (GLMM) with a binomial error structure to analyse the impact of noise colour and temperature synchrony on parasite prevalence during the experiment. The linear term for time was included in this model as a covariate. General linearized models (GLMs) with a binomial error structure were used to analyse variation in the proportion of populations reaching peak prevalence before the end of the experiment, and variation in final parasite prevalence. A GLM with a normal error structure analysed variation in synchrony in prevalence fluctuations between subpopulations. Synchrony in parasite prevalence through time between subpopulations was assessed using the intraclass correlation coefficient (r_i) calculated for each metapopulation [36]. If r_i is close to 1, subpopulations are defined as synchronous; if r_i is close to 0 dynamics are uncorrelated; and if r_i is close to −1 populations are anti-synchronous [36].

(ii) Host dynamics

We used a GLMM with a normal error structure to investigate how parasite infection, noise colour and temperature synchrony influenced *Paramecium* metapopulation size (log-transformed) during the experiment. As above, the model included time as a covariate. In complementary analyses, GLMs with a normal error structure were used to analyse variation in metapopulation decline and synchrony in density fluctuations between subpopulations. The rate of metapopulation decline was taken as the slope of the linear regression of *Paramecium* total population size through time. Subpopulation synchrony was described by the intraclass correlation coefficient of total population density [36].

(iii) Control treatments

We used GLMMs to compare the effects of the constant (5 or 23°C) versus variable temperature treatments (red and white noise combined) on parasite prevalence (binomial error structure). In a similar model, we compared the effect of constant versus variable temperature treatments and parasite infection on *Paramecium* density (normal error structure). Time was included in these models as a covariate. A GLM with a binomial error structure was used to compare peak prevalence in the constant environment at 23°C, with peak prevalence in the temporally variable environments.

In all analyses, the metapopulation was the unit of replication. In GLMM analyses, metapopulation was included in models as a random factor, and mean deviances were used for quasi-*F*-tests. Where necessary, deviances were scaled for overdispersion, so that mean residual deviances were equal to 1. Statistical models were initially fully factorial for temperature treatments (noise colour, temperature synchrony) and parasite infection; they also included migration rate as a main effect. Analyses with time as a covariate contained metapopulation as a nested factor within experimental treatments. All models were simplified by removing non-significant terms ($p > 0.10$). All analyses were conducted with the JMP 10 statistical package [37]. Fitting autoregressive error structures [38] in models including time did not improve model fits, so we retained the simpler models.

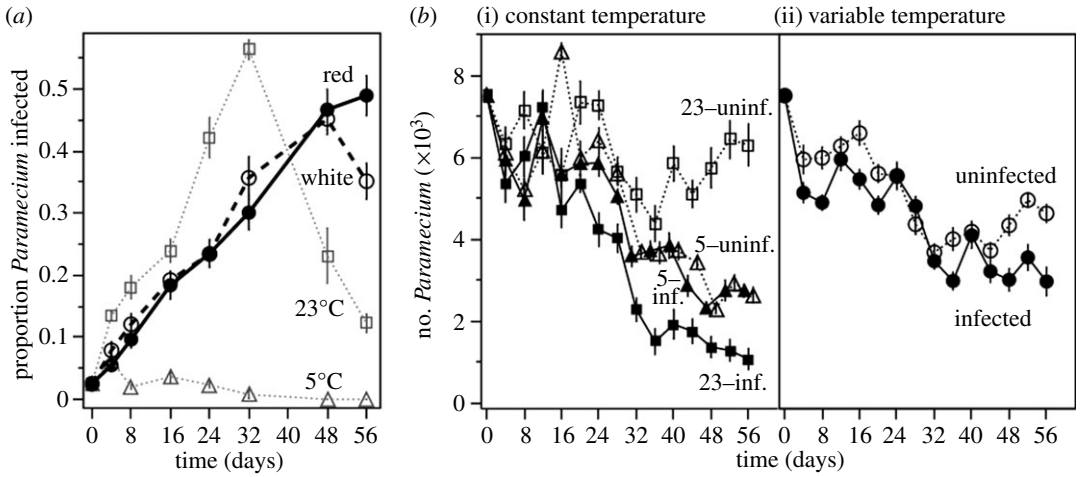

Figure 1. (*a*) Mean (±s.e.) parasite infection prevalence in metapopulations, measured as mean proportion of *Paramecium* infected, in constant (5 and 23°C) and variable (red and white noise) temperature environments. (*b*) Mean *Paramecium* subpopulation sizes in infected (solid lines) and uninfected (dashed lines) metapopulations in (i) constant 5 and 23°C environments and (ii) variable temperature environments.

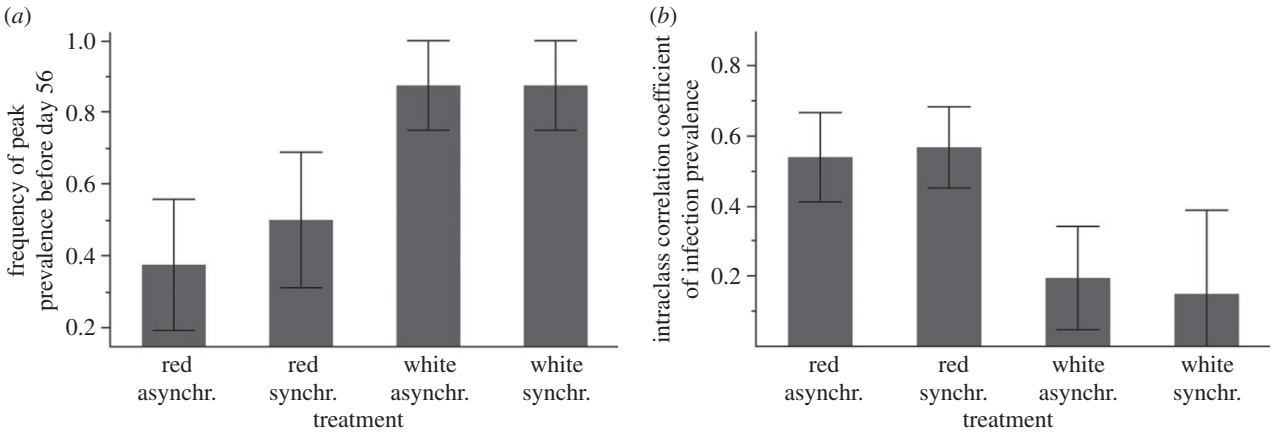

Figure 2. (*a*) Mean (±s.e.) proportion of infected metapopulations reaching peak parasite prevalence before day 56 of the experiment and (*b*) synchrony in parasite infection prevalence fluctuations between subpopulations, for metapopulations experiencing red or white noise, with synchronous or asynchronous temperatures. Synchrony in subpopulation parasite prevalence is measured as the intraclass correlation coefficient (note values close to 1 mean dynamics are synchronous and close to 0 mean uncorrelated).

3. Results

Here, we focus on the effects of noise colour and how it interacted with temperature synchrony to influence parasite spread and *Paramecium* population dynamics. Results on the influence of migration on the spatial aspects of the epidemic will be presented elsewhere. It should be noted that migration did not significantly interact with noise colour for any measure, for either the parasite or the *Paramecium* populations.

(a) Parasite dynamics

(i) Constant versus variable temperatures

The temperature treatments had contrasting effects on parasite prevalence during the experiment (significant time × temperature treatment interaction: $F_{1,335} = 49.28$, $p < 0.0001$; electronic supplementary material, table S1; figure 1*a*). At constant 23°C, prevalence increased from initially 2.5% in the metapopulation to peak levels around 50%, before declining towards the end of the experiment. By contrast, at 5°C, the parasite declined in prevalence and went extinct in all metapopulations. This confirmed that 5°C represented a population sink for the parasite. In the variable temperature treatments, epidemics progressed more slowly than at constant 23°C (figure 1*a*). Consequently, although peak prevalence was the same ($\chi^2_1 = 2.32$, $p = 0.1277$), it was reached almost 20 days earlier at constant 23°C. Thus, recurrent exposure to 5°C delayed parasite spread within variable treatments.

(ii) Variable temperatures: temporal noise colour

Time-series analysis (see electronic supplementary material, table S2) revealed a significant impact of temporal noise structure on parasite prevalence, especially towards the end of the experiment (noise colour × time: $F_{1,225} = 6.60$, $p = 0.01$). Red noise delayed peak parasite prevalence, with maximum infection being observed prior to the end of the experiment (before day 56) in only 43.8% of metapopulations, while peak prevalence was reached in 87% of the metapopulations experiencing white noise (noise colour: $\chi^2_1 = 7.20$, $p = 0.0073$; figure 2*a*). Furthermore, infection declined almost immediately following the peak under white noise, but held constant or continued to increase under red noise (effect of noise colour on final prevalence: $\chi^2_1 = 5.05$, $p = 0.0246$; figure 1*a*). Temperature synchrony did not significantly influence parasite prevalence alone or in combination with noise colour (all main effects and interactions: $p > 0.77$; electronic supplementary material, table S2).

Red noise increased the synchrony in parasite dynamics across the metapopulation (noise colour: $\chi^2_1 = 6.11$, $p = 0.0134$;

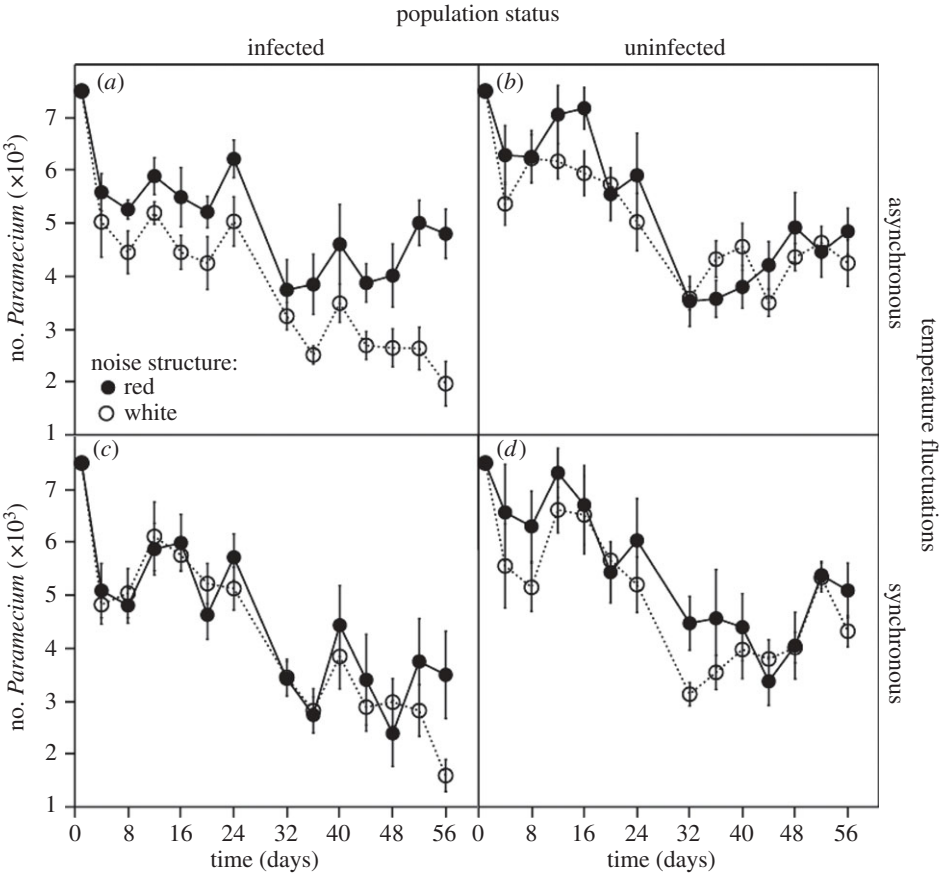

Figure 3. Mean (±s.e.) *Paramecium* subpopulation size for (*a*) infected and (*b*) uninfected metapopulations experiencing asynchronous temperatures, and (*c*) infected and (*d*) uninfected metapopulations experiencing synchronous temperatures under red (closed circles) and white (open circles) noise.

figure 2*b*). This is indicated by the higher mean intraclass correlation coefficient of parasite prevalence dynamics between subpopulations in the red noise environments.

(b) Host dynamics

(i) Constant versus variable temperatures

The impact of parasite infection on metapopulation size varied with temperature treatment (temperature treatment × infection × time interaction: $F_{1,1337} = 63.44$, $p < 0.0001$; electronic supplementary material, table S3). At constant 23°C, infected populations showed a sustained decline during the course of the experiment, whereas the uninfected populations maintained high densities. Constant 5°C treatment resulted in a 50% reduction in uninfected *Paramecium* metapopulation size relative to constant 23°C (figure 1*b*). At constant 5°C, infected populations lost infection and maintained equivalent densities to uninfected populations (figure 1*b*). The variable treatment resulted in the decline of both infected and uninfected populations, but marked differences between these two treatments were most apparent towards the end of the experiment. The mean effect of infection on population densities in variable treatments fell between those of the two constant treatments (see electronic supplementary material, table S2; figure 1*b*).

(ii) Variable temperatures: noise colour and temperature synchrony

The impact of infection on host population dynamics depended on the combined effects of both temporal noise colour and temperature synchrony (significant infection × noise colour × temperature synchrony interaction for *Paramecium* density: $F_{1,56} = 6.2$, $p = 0.0125$; electronic supplementary material, table S4). We found that red noise consistently increased population density over that of white noise for infected populations experiencing asynchronous temperature fluctuations (figures 3*a* and 4*a*). This positive effect was absent or much less pronounced in the other treatment combinations (figures 3*b–d* and 4*a*). The effect of red noise under asynchronous temperatures enabled infected *Paramecium* metapopulations to maintain densities equivalent to uninfected metapopulations (figure 4*a*). This was associated with reduced overall rates of decline for infected populations under red noise that were equivalent to those observed in uninfected populations (infection × noise interaction: $\chi^2_2 = 6.45$, $p = 0.0111$; electronic supplementary material, table S4B; figure 3*a*). Note that neither noise colour nor temperature synchrony had a significant effect on uninfected metapopulations (figure 4*a*).

Furthermore, the combination of red noise and asynchronous temperatures reduced population synchrony in infected metapopulations, compared with uninfected metapopulations. For the other three treatment combinations, we observed the opposite trend, with parasite infection increasing synchrony in metapopulations (temperature synchrony × infection × noise interaction: $\chi^2_2 = 4.69$, $p = 0.0303$; electronic supplementary material, table S4C; figure 4*b*).

4. Discussion

We demonstrated experimentally that the temporal and spatial structure of environmental noise can influence host and parasite dynamics in a metapopulation. Consistent with prevailing

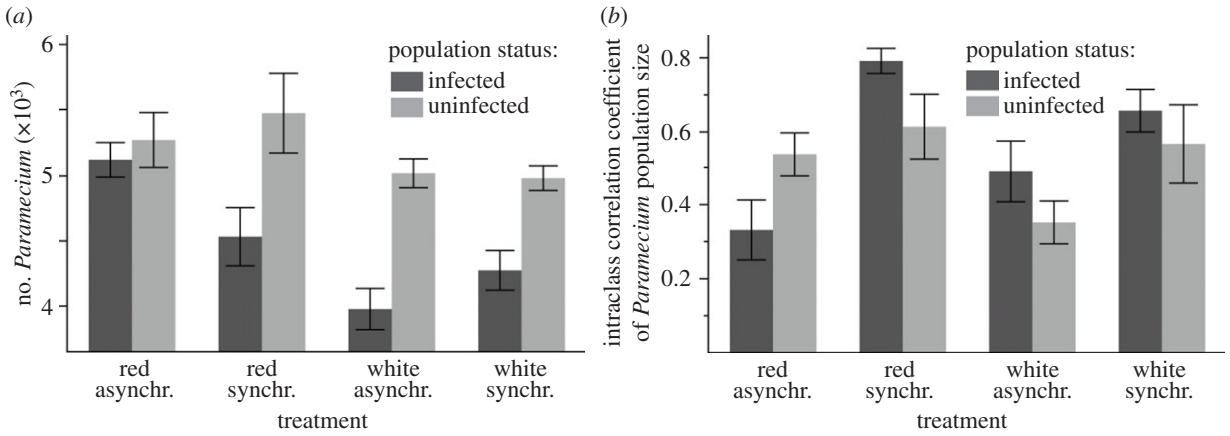

Figure 4. (*a*) Mean subpopulation size during the experiment and (*b*) synchrony in subpopulation density dynamics, shown for infected and uninfected metapopulations exposed to red or white noise, with asynchronous or synchronous temperatures. Synchrony in subpopulation density fluctuations is measured as the intraclass correlation coefficient (note values close to 1 mean dynamics are synchronous and close to 0 mean uncorrelated).

theory [17] that predicts a beneficial effect of red noise, we found that infected *Paramecium* metapopulations benefited from the combined effects of red noise and asynchronous temperatures, enabling them to maintain equivalent population densities to uninfected metapopulations. Red noise also benefited the parasite, increasing synchrony in subpopulation parasite prevalence and enhancing persistence at later stages of the epidemic. It is noteworthy that all populations in the variable treatments spent the same number of days at both 5 and 23°C. The differences between red and white noise treatments would not have been apparent if species' responses to variable environments were an average of their responses to the corresponding constant environments. It is the nonlinear response to stochasticity that underlies the differences in the dynamics between the red and white noise treatments [14].

(a) Parasite

(i) Temporal noise structure and parasite epidemics

Previous theory and experimental work have demonstrated a beneficial effect of red noise on population growth and persistence for sink populations [14]. Our results indicate that this effect extends to the more complex case of parasitic organisms interacting with their host. In our experiment, red noise was characterized by extended periods in both permissive (23°C) and restrictive (5°C) conditions. We hypothesized that while 5°C arrests parasite development, an extended period at 23°C facilitates parasite within-host multiplication and the accumulation of infectious forms [25]. As 23°C also favours host division, this should further boost both vertical and horizontal transmission, because infectious forms are disseminated with each division as well as being transferred to daughter cells. By contrast, white noise entails more frequent environmental changes, with shorter periods of time at each temperature. If there is a lag for parasite development and/or host division, then shorter periods at 23°C should be less conducive to parasite spread. The importance of lag effects on parasite development in the response to environmental stochasticity has been demonstrated [10]. However, our results are better explained by indirect effects of noise structure on the host *Paramecium* populations. We found that red noise drove higher host population densities than white noise towards the end of the experiment (figure 1*a*). Increased *Paramecium* density under red noise may lead to higher host–parasite contact rates and, consequently, higher rates of horizontal parasite transmission [39]. Consequently, enhanced transmission under red noise may have prevented the parasite declines observed under white noise. Consistent with this idea of a density-mediated effect, there was an overall positive relationship between the number of hosts harbouring new infections (a measure of the force of infection; see [40]) and the frequency of infectious hosts (producing infectious forms) in the population ($\chi^2_1 = 18.07, p < 0.0001$). However, the number of new infections detected in our fixed samples was too low for more detailed analyses investigating the effects of red versus white noise.

(ii) Temperature synchrony and parasite spread

We expected synchronous temperatures to synchronize parasite fluctuations in metapopulations. However, this was not the case. The intraclass correlation coefficient, describing the synchrony in prevalence changes, was affected by the temporal noise colour, but not by synchronous temperatures. Indeed, red noise enhanced synchrony in subpopulation fluctuations, a result also observed by Fontaine & Gonzalez [41]. The reason for this result is not clear, but it may be due to indirect effects of red noise on realized migration rates. Migration was implemented through the transfer of a fixed fraction of medium, so higher host densities would result in greater realized migration rates. Increased migration is known to increase synchrony in parasite populations fluctuations [42].

(b) Host

(i) Combined effects of noise and temperature synchrony on *Paramecium* metapopulation dynamics

Our main finding for *Paramecium* populations is that infected metapopulations experiencing both red noise and asynchronous temperatures were able to maintain equivalent population densities to uninfected metapopulations. This is consistent with theory that predicts that spatial heterogeneity enhances the beneficial effect of red noise on population densities in sink metapopulations [17]. Red noise is predicted to permit population recovery during temporary periods in permissive conditions. Asynchronous temperatures cause subpopulations to experience contrasting conditions, so that large subpopulations can rescue small subpopulations. Matthews & Gonzalez [16] found that red noise and asynchronous temperatures permitted higher *Paramecium aurelia* densities in metapopulations.

Interestingly, we replicated only this finding for infected *P. caudatum* populations; uninfected metapopulations were not affected by the structure of the temporal or spatial variation. A previous experiment identified that the beneficial effect of red noise is greater in more severe sink conditions [14]. Here, we used a different *Paramecium* species, for which it might be the case that the relatively warm mean temperatures (14°C) imposed in our fluctuating environments require higher culling to create a severe enough sink to permit a beneficial effect of red noise in the absence of the parasite. Thus, we hypothesize that an indirect effect of parasitism is to sufficiently reduce metapopulation sizes for red noise to have a sink-rescuing effect. Additional experiments that manipulate culling rates and mean temperatures are required to identify the conditions required to observe a beneficial effect of red noise in uninfected *P. caudatum* populations.

(ii) Combined effects of noise and asynchronous temperatures on *Paramecium* subpopulation dynamics

The same combination of red noise and asynchronous temperatures also influenced *Paramecium* dynamics at the subpopulation level. Red noise, coupled with asynchronous temperatures, reduced subpopulation synchrony in the infected metapopulations (figure 4*b*). Asynchronous temperatures are predicted to enhance the beneficial effect of red noise due to a decoupling of dynamics between subpopulations. Theory predicts that asynchronous temperatures allow demographic rescue by migration from a source subpopulation to a sink subpopulation. This decoupling of density dynamics between subpopulations probably enabled the higher population densities observed in our infected metapopulations [17]. This idea is further supported by the negative relationship between the degree of synchrony between subpopulations and mean population size at the level of the metapopulation for infected and uninfected populations (all metapopulations pooled: $r = -0.31$, $n = 64$, $p = 0.01$; electronic supplementary material, figure S2). Thus, metapopulations with a higher degree of asynchrony between subpopulations could maintain higher densities.

(c) Implications

(i) Noise colour is important for the dynamics of an epidemic

Previous time-series analyses have identified that changes in parasite incidence and severity are associated with variation in environmental conditions [5,43,44], and that the inclusion of temporal environmental variation is crucial for accurate prediction of epidemic onset [4]. A number of studies highlight the importance of extrinsic environmental stochasticity for parasite epidemiology [10,19]. However, the precise role of noise colour on dynamics has been largely overlooked (but see [18]). This is despite a number of studies demonstrating that environmental noise structure can impact population persistence in both single- and mixed-species populations [13]. Our study provides additional evidence, and shows environmental noise also influences parasite dynamics and the impact of parasitism on host populations. Our study is especially timely as current trends suggest that environmental autocorrelation is changing with global warming [11,45]. Should climate variation become increasingly reddened [11], we would expect this to influence parasite dynamics. We hope that our study will motivate further theoretical and empirical research investigating the role of noise colour on host–parasite dynamics.

(ii) Parasite spread and disease management

Synchrony in parasite dynamics between subpopulations is expected to have implications for disease management across metapopulations. Parasites that exhibit synchrony in epidemics across metapopulations are thought to be easier to control than those with asynchronous dynamics. Simultaneous vaccination of a parasite with synchronous dynamics is more likely to result in metapopulation-wide eradication [46]. We find that red noise enhances synchrony in dynamics between subpopulations compared with white noise. Thus, across our metapopulations, parasite control or eradication would be more probable under red noise. However, we also identified that red noise is also associated with higher parasite prevalence at the level of the metapopulation. High parasite prevalence may complicate control efforts, suggesting that the link between subpopulation synchrony and metapopulation prevalence should be investigated further.

5. Conclusions

We demonstrated the counterintuitive result that red noise is beneficial for both host and parasite relative to white noise. Red noise enhanced parasite persistence, and enabled infected *Paramecium* populations to maintain population sizes that were equivalent to uninfected populations. These results highlight the importance of environmental noise structure for parasite epidemiology, and the impacts of parasitism on host populations. Our results suggest that models incorporating realistic stochastic fluctuations will improve the prediction of future epidemics. Finally, because climate change is expected to alter noise colour [11], this result has intriguing implications for our understanding of parasite epidemiology over the coming century.

Acknowledgements. We thank Joel Cohen, Pedro Vale, Tom Raffel and two anonymous reviewers for very helpful comments on this manuscript. We also thank Claire Barbera for help in the laboratory.

Funding statement. This work was supported by grants from the Agence National de la Recherche ('ANR-09-BLAN-0099', A.B.D. and O.K.). A.G. is supported by the Canada Research Chair programme. All data have been deposited in Dryad.

References

1. Wolinska J, King KC. 2009 Environment can alter selection in host–parasite interactions. *Trends Parasitol.* **25**, 236–244. (doi:10.1016/j.pt.2009.02.004)
2. Altizer S, Dobson A, Hosseini P, Hudson P, Pascual M, Rohani P. 2006 Seasonality and the dynamics of infectious diseases. *Ecol. Lett.* **9**, 467–484. (doi:10.1111/j.1461-0248.2005.00879.x)
3. Duncan AB, Fellous S, Kaltz O. 2011 Temporal variation in temperature determines disease spread and maintenance in *Paramecium* microcosm populations. *Proc. R. Soc. B* **278**, 3412–3420. (doi:10.1098/rspb.2011.0287)
4. Paaijmans KP, Blanford S, Bell AS, Blanford JI, Read AF, Thomas MB. 2010 Influence of climate on malaria transmission depends on daily temperature

variation. *Proc. Natl Acad. Sci. USA* **107**, 15 135–15 139. (doi:10.1073/pnas.1006422107)

5. Hovmoller MS. 2001 Disease severity and pathotype dynamics of *Puccinia striiformis* f.sp. *tritici* in Denmark. *Plant Pathol.* **50**, 181–189. (doi:10.1046/j.1365-3059.2001.00525.x)
6. Mboup M, Bahri B, Leconte M, De Vallavieille-Pope C, Kaltz O, Enjalbert J. 2012 Genetic structure and local adaptation of European wheat yellow rust populations: the role of temperature-specific adaptation. *Evol. Appl.* **5**, 341–352. (doi:10.1111/j.1752-4571.2011.00228.x)
7. Metcalf CJE, Bjørnstad ON, Grenfell BT, Andreasen V. 2009 Seasonality and comparative dynamics of six childhood infections in pre-vaccination Copenhagen. *Proc. R. Soc. B* **276**, 4111–4118. (doi:10.1098/rspb.2009.1058)
8. Schär C, Vidale PL, Lüthi D, Frei C, Häberli C, Liniger MA, Appenzeller C. 2004 The role of increasing temperature variability in European summer heatwaves. *Nature* **427**, 332–336. (doi:10.1038/nature02300)
9. Rohani P, King AA. 2010 Never mind the length, feel the quality: the impact of long-term epidemiological data sets on theory, application and policy. *Trends Ecol. Evol.* **25**, 611–618. (doi:10.1016/j.tree.2010.07.010)
10. Truscott JE, Gilligan CA. 2003 Response of a deterministic epidemiological system to a stochastically varying environment. *Proc. Natl Acad. Sci. USA* **100**, 9067–9072. (doi:10.1073/pnas.1436273100)
11. Wigley TM. 1998 Anthropogenic influence on the autocorrelation structure of hemispheric-mean temperatures. *Science* **282**, 1676–1679. (doi:10.1126/science.282.5394.1676)
12. Vasseur DA, Yodzis P. 2004 The color of environmental noise. *Ecology* **85**, 1146–1152. (doi:10.1890/02-3122)
13. Ruokolainen L, Lindén A, Kaitala V, Fowler MS. 2009 Ecological and evolutionary dynamics under coloured environmental variation. *Trends Ecol. Evol.* **24**, 555–563. (doi:10.1016/j.tree.2009.04.009)
14. Gonzalez A, Holt RD. 2002 The inflationary effects of environmental fluctuations in source–sink systems. *Proc. Natl Acad. Sci. USA* **99**, 14 872–14 877. (doi:10.1073/pnas.232589299)
15. Bjornstad ON, Ims RA, Lambin X. 1999 Spatial population dynamics: analyzing patterns and processes of population synchrony. *Trends Ecol. Evol.* **14**, 427–432. (doi:10.1016/S0169-5347(99)01677-8)
16. Matthews DP, Gonzalez A. 2007 The inflationary effects of environmental fluctuations ensure the persistence of sink metapopulations. *Ecology* **88**, 2848–2856. (doi:10.1890/06-1107.1)
17. Roy M, Holt RD, Barfield M. 2005 Temporal autocorrelation can enhance the persistence and abundance of metapopulations comprised of coupled sinks. *Am. Nat.* **166**, 245–261. (doi:10.1086/431286)
18. Marion G, Renshaw E, Gibson G. 2000 Stochastic modelling of environmental variation for biological populations. *Theor. Popul. Biol.* **57**, 197–217. (doi:10.1006/tpbi.2000.1450)
19. Rand DA, Wilson HB. 1991 Chaotic stochasticity: a ubiquitous source of unpredictability in epidemics. *Proc. R. Soc. Lond. B* **246**, 179–184. (doi:10.1098/rspb.1991.0142)
20. Raffel TR, Romansic JM, Halstead NT, Mcmahon TA, Venesky MD, Rohr JR. 2012 Disease and thermal acclimation in a more variable and unpredictable climate. *Nat. Clim. Change* **3**, 146–151. (doi:10.1038/NCLIMATE1659)
21. Gallet R, Alizon S, Comte PA, Gutierrez A, Depaulis F, Van Baalen M, Michel E, Muller-Graf CDM. 2007 Predation and disturbance interact to shape prey species diversity. *Am. Nat.* **170**, 143–154. (doi:10.1086/518567)
22. Zhou G, Minakawa N, Githeko AK, Yan G. 2004 Association between climate variability and malaria epidemics in the East African highlands. *Proc. Natl Acad. Sci. USA* **101**, 2375–2380. (doi:10.1073/pnas.0308714100)
23. Constantin de Magny G, Guégan J-F, Petit M, Cazelles B. 2007 Regional-scale climate-variability synchrony of cholera epidemics in West Africa. *BMC Infect. Dis.* **7**, 20. (doi:10.1186/1471-2334-7-20)
24. Huppert A, Barnea O, Katriel G, Yaari R, Roll U, Stone L. 2012 Modeling and statistical analysis of the spatio-temporal patterns of seasonal influenza in Israel. *PLoS ONE* **7**, e45107. (doi:10.1371/journal.pone.0045107)
25. Fels D, Kaltz O. 2006 Temperature-dependent transmission and latency of *Holospora undulata*, a micronucleus-specific parasite of the ciliate *Paramecium caudatum*. *Proc. R. Soc. B* **273**, 1031–1038. (doi:10.1098/rspb.2005.3404)
26. Krenek S, Petzoldt T, Berendonk TU. 2012 Coping with temperature at the warm edge: patterns of thermal adaptation in the microbial eukaryote *Paramecium caudatum*. *PLoS ONE* **7**, e30598. (doi:10.1371/journal.pone.0030598)
27. Wichterman R. 1986 *The biology of Paramecium*. New York, NY: Plenum Press.
28. Nidelet T, Kaltz O. 2007 Direct and correlated responses to selection in a host–parasite system: testing for the emergence of genotype specificity. *Evolution* **61**, 1803–1811. (doi:10.1111/j.1558-5646.2007.00162.x)
29. Lampert UWS. 1999 *Limnoecology*. Stuttgart, Germany: Thieme.
30. Fokin SI. 2004 Bacterial endocytobionts of ciliophora and their interactions with the host cell. *Int. Rev. Cytol.* **236**, 181–249. (doi:10.1016/S0074-7696(04)36005-5)
31. Nidelet T, Koella JC, Kaltz O. 2009 Effects of shortened host life span on the evolution of parasite life history and virulence in a microbial host–parasite system. *BMC Evol. Biol.* **9**, 65. (doi:10.1186/1471-2148-9-65)
32. Duncan AB, Fellous S, Accot R, Alart M, Chantung Sobandi K, Cosiaux A, Kaltz O. 2010 Parasite-mediated protection against osmotic stress for *Paramecium caudatum* infected by *Holospora undulata* is host genotype specific. *FEMS Microbiol. Ecol.* **74**, 353–360. (doi:10.1111/j.1574-6941.2010.00952.x)
33. Magalon H, Nidelet T, Martin G, Kaltz O. 2010 Host growth conditions influence experimental evolution of life history and virulence of a parasite with vertical and horizontal transmission. *Evolution* **64**, 2126–2138. (doi:10.1111/j.1558-5646.2010.00974.x)
34. Restif O, Kaltz O. 2006 Condition-dependent virulence in a horizontally and vertically transmitted bacterial parasite. *Oikos* **114**, 148–158. (doi:10.1111/j.2006.0030-1299.14611.x)
35. Adiba S, Huet M, Kaltz O. 2010 Experimental evolution of local parasite maladaptation. *J. Evol. Biol.* **23**, 1195–1205. (doi:10.1111/j.1420-9101.2010.01985.x)
36. Zar JH. 1999 *Biostatistical analysis*. Upper Saddle River, NJ: Prentice Hall.
37. SAS Institute Inc. 2012 *Jmp In, version 10.1*. Cary, NC: SAS Institute.
38. Pollitt LC, Reece SE, Mideo N, Nussey DH, Colegrave N. 2012 The problem of auto-correlation in parasitology. *PLoS Pathog.* **8**, e1002590. (doi:10.1371/journal.ppat.1002590)
39. Lopez-Pascua LDC, Buckling A. 2008 Increasing productivity accelerates host–parasite coevolution. *J. Evol. Biol.* **21**, 853–860. (doi:10.1111/j.1420-9101.2008.01501.x)
40. Fellous S, Duncan AB, Quillery E, Vale PF, Kaltz O. 2012 Genetic influence on disease spread following arrival of infected carriers. *Ecol. Lett.* **15**, 186–192. (doi:10.1111/j.1461-0248.2011.01723.x)
41. Fontaine C, Gonzalez A. 2005 Population synchrony induced by resource fluctuations and dispersal in an aquatic microcosm. *Ecology* **86**, 1463–1471. (doi:10.1890/04-1400)
42. Dey S, Joshi A. 2006 Stability via asynchrony in *Drosophila* metapopulations with low migration rates. *Science* **312**, 434–436. (doi:10.1126/science.1125317)
43. Ruiz MO, Chaves LF, Hamer GL, Sun T, Brown WM, Walker ED, Haramis L, Goldberg TL, Kitron UD. 2010 Local impact of temperature and precipitation on West Nile virus infection in *Culex* species mosquitoes in northeast Illinois, USA. *Parasites Vectors* **3**, 19. (doi:10.1186/1756-3305-3-19)
44. Koelle K, Rodó X, Pascual M, Yunus M, Mostafa G. 2005 Refractory periods and climate forcing in cholera dynamics. *Nature* **436**, 696–700. (doi:10.1038/nature03820)
45. García-Carreras B, Reuman DC. 2011 An empirical link between the spectral colour of climate and the spectral colour of field populations in the context of climate change. *J. Anim. Ecol.* **80**, 1042–1048. (doi:10.1111/j.1365-2656.2011.01833.x)
46. Earn DJ, Rohani P, Grenfell BT. 1998 Persistence, chaos and synchrony in ecology and epidemiology. *Proc. R. Soc. Lond. B* **265**, 7–10. (doi:10.1098/rspb.1998.0256)